Improved Theory for the Temperature-Dependent Hyperfine Coupling Constant of Rare-Earth S-State Ions*

T. J. MENNE

Research Division, McDonnell Douglas Corporation, St. Louis, Missouri 63166

An improved version of the theory for the temperature dependence of the hyperfine coupling constant of rare-earth S-state ions in cubic crystals is developed which incorporates an exact spatial-averaging procedure valid over the entire phonon-wavelength range. The improved treatment eliminates one of the major weaknesses and points of uncertainty in the theory, viz., the ambiguity arising from the existence of separate calculations applicable only in the long- or short-wavelength limits. The question of the range of validity of these approximations is therefore removed. Contributions from both the acoustic branch, based on a Debye spectrum, and the optical branches, based on an Einstein spectrum, are determined. It is shown that the new expressions reduce exactly to those obtained in the long-wavelength limit, but not to those commonly associated with the short-wavelength approximation. The improved theory is applied to the temperature dependence of the hyperfine coupling constant of $^{151}Eu^{2+}$ in CaF_2, SrF_2, and BaF_2, and the results are compared with those of the long-wavelength model as well as with the experimental data. Good qualitative agreement with experiment is obtained, and possible sources of the disagreement between the observed magnitude of the temperature decrease in the hyperfine constant and that predicted by the improved theory are discussed. In addition, calculations of the rigid-lattice values of the hyperfine constant of Eu^{2+} are made, and it is found that these values are not equal in the alkaline-earth fluorides, the differences lying outside the error limits. Finally, the improved treatment shows that some of the results produced by the long-wavelength approximation are in fact spurious.

I. INTRODUCTION

THE orbit-lattice interaction V_{OL} describes the influence of the phonon field on the orbital motion of electrons in impurity ions. It has been successfully applied to the study of spin-lattice relaxation times of ions in crystals by Van Vleck[1] and by Orbach.[2] Although it plays a negligible role in the crystal field splitting of S-state ions,[3,4] the orbit-lattice interaction has a pronounced effect on the temperature dependence of the hyperfine coupling constant of these ions. Šimánek and Orbach[5] first demonstrated this effect for the MgO:Mn^{2+} system. Their calculation was based on the long-wavelength approximation, i.e., $kR \ll 1$, where k is the phonon wave vector and R is the interionic distance. Good qualitative agreement with experiment was obtained, but Huang[6] later argued that the long-wavelength approximation was not appropriate for the high-temperature region. He then applied the theory to Mn^{2+} in alkali halides using the opposite approximation, i.e., $kR \gg 1$, and also obtained good agreement with the data. It is interesting to note that both approximations have also been used in the analyses of spin-lattice relaxation data.[1,7] Consequently, an ambiguity has developed in the general theory of the orbit-lattice interaction, since calculations may be performed using either the long- or the short-wavelength approximations. The validity of the results obtained from these calculations is neces-

sarily questionable, since the temperature range over which either of these opposing approximations is valid is not known.

Calculations based on the long- or short-wavelength approximation encounter other difficulties as well. Both the acoustic and optical branches of the phonon spectrum should, of course, be included in such calculations. Generally, one considers the acoustic branch only and employs the approximation $kR \ll 1$, but calculations including both acoustic and optical branches using $kR \gg 1$ have also been performed.[6] Some portions of the phonon spectrum are necessarily excluded in treatments involving any of these approximations, and of course the region $kR \approx 1$ has never been treated at all. In addition, it is commonly found[8] that orbit-lattice calculations which invoke the point-charge model yield magnitudes of the coefficients which are considerably smaller than the experimentally observed values. It is important to know how much of this discrepancy can be attributed to the use of the long- or short-wavelength approximations.

It is the purpose of this paper to present a calculation of the temperature dependence of the hyperfine coupling constant for rare-earth ions which includes an exact treatment of the phonon wavelength. Spatial averaging over products of the normal coordinates of the molecular cluster, which has previously been accomplished only by utilizing the long- and short-wavelength approximations, is achieved here by expanding the normal coordinates in spherical Bessel functions so that the spatial averaging is valid over the entire phonon-wavelength range. The analytical expressions obtained are sufficiently simple so that there is no longer any advantage to performing the calculation in either the long- or

[1] J. H. Van Vleck, Phys. Rev. **57**, 426 (1940).
[2] R. Orbach, Proc. Roy. Soc. (London) **A264**, 458 (1961).
[3] T. J. Menne, J. Phys. Chem. Solids **28**, 1629 (1967).
[4] T. J. Menne, Phys. Rev. **170**, 356 (1968).
[5] E. Šimánek and R. Orbach, Phys. Rev. **145**, 191 (1966).
[6] C. Y. Huang, Phys. Rev. **158**, 280 (1967).
[7] C. Y. Huang, Phys. Rev. **154**, 215 (1967).
[8] M. Blume and R. Orbach, Phys. Rev. **127**, 1587 (1966).

short-wavelength limits. Moreover, it is shown that the new calculation correctly reduces to the expressions obtained previously by Menne, Ames, and Lee[9] in the limit $kR \ll 1$.

Both the acoustic and optical branches are included in the calculation and are treated by means of the Debye and Einstein approximations, respectively. Then the improved theory is applied to the analysis of the temperature-dependent hyperfine constant $A(T)$, as well as its rigid-lattice value A_{RL}, for the Eu^{2+} in CaF_2, SrF_2, and BaF_2 data.[9,10] Results of this analysis are compared with those obtained from the long-wavelength theory.

We wish to emphasize that, besides the use of approximations concerning the phonon wavelength, there exist other weaknesses in the present theory for the temperature dependence of the hyperfine constant for both iron-group and rare-earth ions, e.g., use of the point-charge model with covalency and overlap neglected,[11] inclusion of nearest neighbors only, use of a constant Debye temperature over an 800°K temperature range, neglect of local modes, and use of improper lattice eigenvectors of the host crystal. Seeking to improve the theory, and in order to evaluate the zero-point phonon contribution to the hyperfine field, Orbach and co-workers[12,13] invoked a linear diatomic chain model of the lattice which enabled them to treat both the acoustic and optical branches of the spectrum. Their approach represents an improvement with respect to effects arising from the entire crystal lattice, whereas our exact treatment of the phonon wavelength represents an improvement in the treatment of effects arising from the local environment of the rare-earth ion. Thus, we believe that the exact phonon-wavelength method presented here is a significant advance over the approximate treatments and serves to remove one of the major weaknesses and points of uncertainty in the model. Further improvements in the theory are desirable but difficult to achieve at this time.

A similar calculation for the temperature-dependent hyperfine coupling constant of the iron-group S-state ions is being performed and will be reported shortly.

II. IMPROVED CALCULATION

A. Spatial Averaging

The model describing the effect of lattice vibrations on the hyperfine field of rare-earth ions possessing a half-filled $4f$ shell ($^8S_{7/2}$ ground state) in a cubic environment was developed in Ref. 9 and is equally valid here. We admixed excited ns orbitals ($n \geq 6$) into the ground $4f$ orbitals by a first-order perturbation in the orbit-

lattice interaction V_{OL} and then calculated the matrix element of the contact hyperfine operator in the perturbed ground state $|^8S',M_S\rangle$. The result is given by Eq. (14) of Ref. 9 in terms of the 10 antisymmetrical normal coordinates q_i of the XY_8 molecular cluster depicted in Fig. 1 of that reference. When the ionic displacements $Q_j{}^\alpha$ are expanded in lattice waves,[14] one obtains

$$Q_j{}^\alpha = 2 \sum_{k,\sigma} P_{k\sigma} \Phi_{\alpha k}{}^\sigma \cos k \cdot R_j{}^0, \qquad (1)$$

where

$$P_{k\sigma} = (\hbar/2\omega_{k\sigma}M)^{1/2}(a_k e^{ik \cdot l_i{}^0} + a_k{}^\dagger e^{-ik \cdot l_i{}^0}), \qquad (2)$$

and where all symbols have been defined in Ref. 9.

It is necessary now to evaluate the average hyperfine field $\langle H_{hyp} \rangle$ by calculating the average over all directions in k space of quantities like

$$\langle \Phi_{\alpha k}{}^\sigma \Phi_{\beta k}{}^\sigma \cos k \cdot R_j{}^0 \cos k \cdot R_l{}^0 \rangle \equiv \langle \alpha,\beta,j,l \rangle_\sigma, \qquad (3)$$

where α and β are any of x, y, and z, and j and l are any of 1, 2, 3, and 4, while σ denotes either the longitudinal (l) or transverse (t) mode. Note that $\langle \alpha,\beta,j,l \rangle$ is symmetric in α and β and in j and l. In the past, this averaging has been accomplished by making either (a) the long-wavelength approximation, i.e., $k \cdot R_j{}^0 \ll 1$, and expanding the cosine to first order in kR for the iron-group ions[1] (even normal coordinates) and to second order in kR for the rare-earth ions[9] (odd normal coordinates), or (b) the short-wavelength approximation, i.e., $k \cdot R_j{}^0 \gg 1$, and treating the quantity in Eq. (3) as a constant[6,7] (independent of k). However, it is possible to perform the spatial average in Eq. (3) exactly by making use[15] of the following expansion[16] in spherical Bessel functions j_n and spherical harmonics $Y_n{}^m$:

$$e^{ik \cdot R} = 4\pi \sum_{n=0}^{\infty} i^n j_n(kR) \sum_{m=-n}^{n} Y_n{}^m(\theta_k,\phi_k) Y_n{}^{m*}(\theta_R,\phi_R), \qquad (4)$$

where θ_F and ϕ_F are the polar and azimuthal angles of the vector F. Then we find that

$$\cos k \cdot R_j{}^0 \cos k \cdot R_l{}^0 = 2\pi \sum_{n=0}^{\infty} \sum_{m=-2n}^{2n} i^{2n} Y_{2n}{}^m(\theta_k,\phi_k)$$
$$\times [j_{2n}(kR_+) Y_{2n}{}^{m*}(\theta_{R_+},\phi_{R_+})$$
$$+ j_{2n}(kR_-) Y_{2n}{}^{m*}(\theta_{R_-},\phi_{R_-})], \qquad (5)$$

in which

$$R_\pm \equiv R_j{}^0 \pm R_l{}^0. \qquad (6)$$

As an example, consider the quantity $\langle x,y,1,3 \rangle_l$ for the longitudinal mode. We have

$$\Phi_{xk}{}^l = \sin\theta_k \cos\phi_k, \quad \Phi_{yk}{}^l = \sin\theta_k \sin\phi_k, \qquad (7)$$

[9] T. J. Menne, D. P. Ames, and Sook Lee, Phys. Rev. **169**, 333 (1968).

[10] Sook Lee, D. P. Ames, and T. J. Menne, Phys. Letters **28A**, 369 (1968).

[11] E. Šimánek and Nai Li Huang, Phys. Rev. Letters **17**, 699 (1966).

[12] R. Orbach and E. Šimánek, Phys. Rev. **158**, 310 (1967).

[13] R. Calvo and R. Orbach, Phys. Rev. **164**, 284 (1967).

[14] M. Born and K. Huang, *Dynamical Theory of Crystal Lattices* (Oxford University Press, London, 1954).

[15] The author is grateful to Dr. J. G. Broerman for pointing out the potential utility of this expansion in performing the directional averages.

[16] L. I. Schiff, *Quantum Mechanics* (McGraw-Hill Book Co., New York, 1955).

TABLE I. Spatial averages of the quantities $\langle \alpha,\beta,j,l\rangle_\sigma$ in Eq. (3) for both the longitudinal and transverse modes.

α,β	j,l	$\langle \alpha,\beta,j,l\rangle_\sigma$ Longitudinal	Transverse
x,y	1,2; 1,4	0	0
	2,3; 3,4	0	0
	1,3	$-\tfrac{1}{4}j_2(\rho_1)$	$\tfrac{1}{8}j_2(\rho_1)$
	2,4	$\tfrac{1}{4}j_2(\rho_1)$	$-\tfrac{1}{8}j_2(\rho_1)$
	1,1; 3,3	$-\tfrac{1}{6}j_2(\rho_3)$	$\tfrac{1}{12}j_2(\rho_3)$
	2,2; 4,4	$\tfrac{1}{6}j_2(\rho_3)$	$-\tfrac{1}{12}j_2(\rho_3)$
x,z	1,3; 1,4	0	0
	2,3; 2,4	0	0
	1,2	$\tfrac{1}{4}j_2(\rho_1)$	$-\tfrac{1}{8}j_2(\rho_1)$
	3,4	$-\tfrac{1}{4}j_2(\rho_1)$	$\tfrac{1}{8}j_2(\rho_1)$
	1,1; 2,2	$\tfrac{1}{6}j_2(\rho_3)$	$-\tfrac{1}{12}j_2(\rho_3)$
	3,3; 4,4	$-\tfrac{1}{6}j_2(\rho_3)$	$\tfrac{1}{12}j_2(\rho_3)$
y,z	1,2; 1,3	0	0
	2,4; 3,4	0	0
	1,4	$\tfrac{1}{4}j_2(\rho_1)$	$-\tfrac{1}{8}j_2(\rho_1)$
	2,3	$-\tfrac{1}{4}j_2(\rho_1)$	$\tfrac{1}{8}j_2(\rho_1)$
	1,1; 4,4	$\tfrac{1}{6}j_2(\rho_3)$	$-\tfrac{1}{12}j_2(\rho_3)$
	2,2; 3,3	$-\tfrac{1}{6}j_2(\rho_3)$	$\tfrac{1}{12}j_2(\rho_3)$
x,x	1,2; 1,3; 2,4; 3,4}	$\{\tfrac{1}{6}j_2(\rho_2)-\tfrac{1}{12}j_2(\rho_1)+\tfrac{1}{6}[j_0(\rho_1)+j_0(\rho_2)]\}$	$\{-\tfrac{1}{12}j_2(\rho_2)+(1/24)j_2(\rho_1)+\tfrac{1}{6}[j_0(\rho_1)+j_0(\rho_2)]\}$
	1,4; 2,3	$\{\tfrac{1}{6}j_2(\rho_1)-\tfrac{1}{3}j_2(\rho_2)+\tfrac{1}{6}[j_0(\rho_1)+j_0(\rho_2)]\}$	$\{-\tfrac{1}{12}j_2(\rho_1)+\tfrac{1}{6}j_2(\rho_2)+\tfrac{1}{6}[j_0(\rho_1)+j_0(\rho_2)]\}$
	1,1; 2,2; 3,3; 4,4}	$\tfrac{1}{6}[1+j_0(\rho_3)]$	$\tfrac{1}{6}[1+j_0(\rho_3)]$
y,y	1,3; 1,4; 2,3; 2,4}	$\{\tfrac{1}{6}j_2(\rho_2)-\tfrac{1}{12}j_2(\rho_1)+\tfrac{1}{6}[j_0(\rho_1)+j_0(\rho_2)]\}$	$\{-\tfrac{1}{12}j_2(\rho_2)+(1/24)j_2(\rho_1)+\tfrac{1}{6}[j_0(\rho_1)+j_0(\rho_2)]\}$
	1,2; 3,4	$\{\tfrac{1}{6}j_2(\rho_1)-\tfrac{1}{3}j_2(\rho_2)+\tfrac{1}{6}[j_0(\rho_1)+j_0(\rho_2)]\}$	$\{-\tfrac{1}{12}j_2(\rho_1)+\tfrac{1}{6}j_2(\rho_2)+\tfrac{1}{6}[j_0(\rho_1)+j_0(\rho_2)]\}$
	1,1; 2,2; 3,3; 4,4}	$\tfrac{1}{6}[1+j_0(\rho_3)]$	$\tfrac{1}{6}[1+j_0(\rho_3)]$
z,z	1,2; 1,4; 2,3; 3,4}	$\{\tfrac{1}{6}j_2(\rho_2)-\tfrac{1}{12}j_2(\rho_1)+\tfrac{1}{6}[j_0(\rho_1)+j_0(\rho_2)]\}$	$\{-\tfrac{1}{12}j_2(\rho_2)+(1/24)j_2(\rho_1)+\tfrac{1}{6}[j_0(\rho_1)+j_0(\rho_2)]\}$
	1,3; 2,4	$\{\tfrac{1}{6}j_2(\rho_1)-\tfrac{1}{3}j_2(\rho_2)+\tfrac{1}{6}[j_0(\rho_1)+j_0(\rho_2)]\}$	$\{-\tfrac{1}{12}j_2(\rho_1)+\tfrac{1}{6}j_2(\rho_2)+\tfrac{1}{6}[j_0(\rho_1)+j_0(\rho_2)]\}$
	1,1; 2,2; 3,3; 4,4}	$\tfrac{1}{6}[1+j_0(\rho_3)]$	$\tfrac{1}{6}[1+j_0(\rho_3)]$

so that

$$\Phi_{xk}{}^l \Phi_{yk}{}^l = \sin^2\theta_k \sin\phi_k \cos\phi_k$$

$$= -\frac{i}{4}\left(\frac{4\pi}{5}\right)^{1/2}\left(\frac{8}{3}\right)^{1/2}(Y_2{}^2 - Y_2{}^{-2}). \quad (8)$$

Now

$$\langle x,y,1,3\rangle_l$$

$$= \frac{1}{4\pi}\int_0^\pi \int_0^{2\pi} \Phi_{xk}{}^l \Phi_{yk}{}^l \cos k\cdot R_1{}^0 \cos k\cdot R_3{}^0 \sin\theta_k d\theta_k d\phi_k$$

$$= \tfrac{1}{2}\sum_{n=0}^\infty \sum_{m=-2n}^{2n} i^{2n}[j_{2n}(kR_+)Y_{2n}{}^{m*}(\theta_{R_+},\phi_{R_+})$$

$$+ j_{2n}(kR_-)Y_{2n}{}^{m*}(\theta_{R_-},\phi_{R_-})]A_l{}^{xy}(n,m), \quad (9)$$

where

$$A_l{}^{xy}(n,m) = \int_0^\pi \int_0^{2\pi} \Phi_{xk}{}^l \Phi_{yk}{}^l Y_{2n}{}^m(\theta_k,\phi_k)$$

$$\times \sin\theta_k \, d\theta_k d\phi_k. \quad (10)$$

The quantity in Eq. (10) can easily be evaluated by substituting for $\Phi_{xk}{}^l \Phi_{yk}{}^l$ from Eq. (8) and by making use of the orthogonality properties of the $Y_n{}^m$. In this manner

the number of terms in the summation of Eq. (9) is also severely restricted, and hence we finally obtain

$$\langle x,y,1,3\rangle_l = -\tfrac{1}{4}j_2[(8/3)^{1/2}kR], \quad (11)$$

in which R is the rare-earth-ion-to-ligand distance.

In a similar manner we have evaluated all of the averages $\langle \alpha,\beta,j,l\rangle_\sigma$ for both the longitudinal and transverse modes, and they are recorded in Table I. Use has been made of the following definitions:

$$\rho_0 = kR, \quad \rho_1 = (8/3)^{1/2}kR, \quad \rho_2 = (\sqrt{\tfrac{4}{3}})kR, \quad \rho_3 = 2kR. \quad (12)$$

To treat the displacements α_N of the central (rare-earth) ion, we first note that

$$\alpha_N = \sum_{k,\sigma} P_{k\sigma}\Phi_{\alpha k}{}^\sigma, \quad (13)$$

so that

$$\langle |\alpha_N|^2\rangle_\sigma = \tfrac{1}{3}\sum_{k,\sigma} |P_{k\sigma}|^2 \quad (14)$$

for all $\alpha = x$, y, z and $\sigma = l$ or t. It remains then to determine the averages

$$\langle Q_i{}^\beta \alpha_N\rangle_\sigma = \langle Q_i{}^\alpha \beta_N\rangle_\sigma, \quad (15)$$

and these are presented in Table II in units of $\sum_{k,\sigma} |P_{k\sigma}|^2$.

B. Final Expressions

There are three acoustic modes for each k, and $3n-3$ optical modes, where n is the number of atoms per unit cell. To include all branches but maintain the total number of modes fixed, any function $f(\omega_\sigma, k_\sigma)$ must be summed over N_c values of k, where N_c is the number of unit cells in a crystal of volume V, for each polarization direction in every branch. Replacing this sum by an integration yields the following operation for each branch:

$$\sum_{\sigma=1}^{3}\sum_{k}^{N_c} f(\omega_{k\sigma}, k_\sigma) = \frac{V}{2\pi^2}\sum_{\sigma=1}^{3}\int_0^{k_D} f_\sigma(k)k^2 dk, \quad (16)$$

where

$$k_D = (6\pi^2 N_c/V)^{1/3} = (6\pi^2 N/nV)^{1/3}, \quad (17)$$

N is the total number of atoms, and where $\omega_{k\sigma}$ was eliminated by means of the dispersion relation appropriate to the branch in question.

Acoustic branch. A Debye spectrum and the dispersion relation $\omega_{k\sigma} = v_\sigma k$, where v_σ is the velocity of sound for the σth mode, are used for the acoustic branch. Since the experimental value of the Debye temperature Θ is

TABLE II. Spatial averages of the quantities $\langle Q_i{}^\alpha \beta_N \rangle_\sigma$ in Eq. (15) in terms of $\sum_{k,\sigma} |P_{k\sigma}|^2$.

α,β	i	$\langle Q_i{}^\alpha\beta_N\rangle_\sigma$ Longitudinal	Transverse
x,y	1; 3	$-\frac{2}{3}j_2(\rho_0)$	$\frac{1}{3}j_2(\rho_0)$
	2; 4	$\frac{2}{3}j_2(\rho_0)$	$-\frac{1}{3}j_2(\rho_0)$
x,z	1; 2	$\frac{2}{3}j_2(\rho_0)$	$-\frac{1}{3}j_2(\rho_0)$
	3; 4	$-\frac{2}{3}j_2(\rho_0)$	$\frac{1}{3}j_2(\rho_0)$
y,z	1; 4	$\frac{2}{3}j_2(\rho_0)$	$-\frac{1}{3}j_2(\rho_0)$
	2; 3	$-\frac{2}{3}j_2(\rho_0)$	$\frac{1}{3}j_2(\rho_0)$
α,α	i	$\frac{2}{3}j_0(\rho_0)$	$\frac{2}{3}j_0(\rho_0)$
(all α)	(all i)		

generally determined by assuming that the entire phonon spectrum can be described by a Debye distribution, we must employ, from Eq. (17), the value of the "reduced Debye temperature" Θ' given by

$$\Theta' = \Theta/n^{1/3}. \quad (18)$$

We can now evaluate Eq. (14) of Ref. 9 by means of Tables I and II and by recalling that only those cross-product terms between normal coordinates transforming like the same component of the repeated Γ_{4u} irreducible representation are nonzero. Then we find

$$\langle H_{\mathrm{hyp}} \rangle = \frac{8\pi}{3} g\mu_B S^z \left(\frac{ee'}{R^5}\right)^2 \sum_{n,n'} U_{nn'} \frac{1496\hbar}{5103\rho\pi^2}\left(\frac{k_B T}{\hbar}\right)^2 \int_0^{\Theta'/T}\left(\frac{2}{e^x-1}+1\right)$$

$$\times \left\{\frac{1}{v_l{}^3}\left[1 + \frac{16}{187}\left(5j_2(\rho_0{}^l) - \frac{7}{9}j_0(\rho_0{}^l)\right) + \frac{3}{2618}\left(755j_2(\rho_1{}^l) - \frac{7462}{9}j_0(\rho_1{}^l)\right)\right.\right.$$

$$\left.- \frac{1}{1309}\left(720j_2(\rho_2{}^l) + \frac{3731}{3}j_0(\rho_2{}^l)\right) - \frac{1}{1309}\left(655j_2(\rho_3{}^l) - \frac{11\,389}{9}j_0(\rho_3{}^l)\right)\right] + \frac{2}{v_t{}^3}\left[1 - \frac{16}{187}\left(\frac{5}{2}j_2(\rho_0{}^t) + \frac{7}{9}j_0(\rho_0{}^t)\right)\right.$$

$$\left.\left.- \frac{3}{2618}\left(\frac{755}{2}j_2(\rho_1{}^t) + \frac{7462}{9}j_0(\rho_1{}^t)\right) + \frac{1}{1309}\left(360j_2(\rho_2{}^t) - \frac{3731}{3}j_0(\rho_2{}^t)\right) + \frac{1}{1309}\left(\frac{655}{2}j_2(\rho_3{}^t) + \frac{11\,389}{9}j_0(\rho_3{}^t)\right)\right]\right\} x dx, \quad (19)$$

where

$$\rho_0{}^\sigma = \kappa^\sigma x, \quad \rho_1{}^\sigma = (8/3)^{1/2}\kappa^\sigma x, \quad \rho_2{}^\sigma = (\tfrac{4}{3})^{1/2}\kappa^\sigma x, \quad \rho_3{}^\sigma = 2\kappa^\sigma x, \quad (20)$$

$$\kappa^\sigma = Rk_B T/v_\sigma\hbar, \quad x = \hbar\omega/k_B T, \quad (21)$$

and $\sigma = l$ or t. We have also defined

$$U_{nn'} \equiv \frac{\langle R_{4f}|r^3|R_{ns}\rangle\langle R_{n's}|r^3|R_{4f}\rangle}{[E(4f)-E(ns)][E(4f)-E(n's)]}\langle\psi_{ns}|\delta(r)|\psi_{n's}\rangle. \quad (22)$$

The zero-point contribution can be integrated exactly, so that we finally obtain for the hyperfine constant

$$A(T) = A(0)\{1 - [F_{ac}{}^0 + F_{ac}(T)]\}. \quad (23)$$

The thermal acoustic-phonon contribution is

$$F_{ac}(T) = D_{ac}T^2(I_l + I_t), \quad (24)$$

$$I_l = \left(\frac{v_l}{v_l}\right)^3\int_0^{\Theta'/T}\left[1 + \frac{16}{187}\left(5j_2(\rho_0{}^l) - \frac{7}{9}j_0(\rho_0{}^l)\right) + \frac{3}{2618}\left(755j_2(\rho_1{}^l) - \frac{7462}{9}j_0(\rho_1{}^l)\right)\right.$$

$$\left.- \frac{1}{1309}\left(720j_2(\rho_2{}^l) + \frac{3731}{3}j_0(\rho_2{}^l)\right) - \frac{1}{1309}\left(655j_2(\rho_3{}^l) - \frac{11\,389}{9}j_0(\rho_3{}^l)\right)\right]\frac{x dx}{e^x-1}, \quad (25)$$

$$I_t = 2 \int_0^{\Theta'/T} \left[1 - \frac{16}{187}\left(\tfrac{5}{2}j_2(\rho_0{}^t) + \frac{7}{9}j_0(\rho_0{}^t)\right) - \frac{3}{2618}\left(\frac{755}{2}j_2(\rho_1{}^t) + \frac{7462}{9}j_0(\rho_1{}^t)\right) \right.$$

$$\left. + \frac{1}{1309}\left(360 j_2(\rho_2{}^t) - \frac{3731}{3}j_0(\rho_2{}^t)\right) + \frac{1}{1309}\left(\frac{655}{2}j_2(\rho_3{}^t) + \frac{11\,389}{9}j_0(\rho_3{}^t)\right) \right] \frac{x\,dx}{e^x - 1}, \quad (26)$$

and the zero-point acoustic-phonon contribution is

$$F_{\mathrm{ac}}{}^0 = \frac{D_{\mathrm{ac}}}{2}\left(\frac{\Theta'}{z}\right)^2 v_t{}^3 \left[\left(\frac{1}{2v_l{}^3} + \frac{1}{v_t{}^3}\right)z^2 - \frac{1}{1309}\left(\frac{608}{v_l} + \frac{23\,213}{8v_t}\right) + \frac{16}{1683}\left(\frac{52}{v_l}\cos z_0{}^l - \frac{31}{v_t}\cos z_0{}^t\right) - \frac{240}{187z}(\sin z_0{}^l - \sin z_0{}^t) \right.$$

$$+ \frac{1}{20\,944}\left(\frac{14\,257}{v_l}\cos z_1{}^l + \frac{8129}{v_t}\cos z_1{}^t\right) - \frac{20\,385}{20\,944 v_t z_1{}^t}(\sin z_1{}^l - \sin z_1{}^t) + \frac{1}{5236}\left(\frac{1571}{v_l}\cos z_2{}^l + \frac{9622}{v_t}\cos z_2{}^t\right)$$

$$\left. + \frac{1620}{1309 v_t z_2{}^t}(\sin z_2{}^l - \sin z_2{}^t) - \frac{1}{47\,124}\left(\frac{17\,284}{v_l}\cos z_3{}^l + \frac{16\,883}{v_t}\cos z_3{}^t\right) + \frac{1965}{5236 v_t z_3{}^t}(\sin z_3{}^l - \sin z_3{}^t) \right]. \quad (27)$$

The subscripted z's are given by

$$z_0{}^\sigma = z/v_\sigma, \qquad z_1{}^\sigma = (8/3)^{1/2}z/v_\sigma,$$
$$z_2{}^\sigma = (\tfrac{4}{3})^{1/2}z/v_\sigma, \qquad z_3{}^\sigma = 2z/v_\sigma, \qquad (28)$$

and unsubscripted z is defined as

$$z \equiv R k_B \Theta'/\hbar. \quad (29)$$

The constant D_{ac} in Eqs. (24) and (27) is

$$D_{\mathrm{ac}} = \frac{8\pi}{3}\frac{g\mu_B \langle S_z\rangle}{H_c}\left(\frac{ee'}{R^5}\right)^2 \sum_{n,n'} U_{nn'} \frac{2992\hbar}{5103\rho\pi^2 v_t{}^3}\left(\frac{k_B}{\hbar}\right)^2, \quad (30)$$

in units of $(^\circ\mathrm{K})^{-2}$.

Optical branch. An Einstein spectrum and the constant-frequency dispersion relations $\omega_{kl} = \omega_l$ and $\omega_{kt} = \omega_t$ are used for the optical branches. Then for each optical branch we find for the hyperfine constant

$$A(T) = A(0)\{1 - [F_{\mathrm{op}}{}^0 + F_{\mathrm{op}}(T)]\}. \quad (31)$$

The thermal optical-phonon contribution is

$$F_{\mathrm{op}}(T) = D_{\mathrm{op}}\left[\left(\frac{\omega_t/\omega_l}{e^{\hbar\omega_l/k_B T} - 1} + \frac{2}{e^{\hbar\omega_t/k_B T} - 1}\right)L_1 \right.$$

$$\left. + \left(\frac{\omega_t/\omega_l}{e^{\hbar\omega_l/k_B T} - 1} - \frac{1}{e^{\hbar\omega_t/k_B T} - 1}\right)L_2 \right], \quad (32)$$

$$L_1 = \frac{y_D{}^2}{1683}\{1122 y_D - 224 j_1(y_D)$$

$$- (\sqrt{\tfrac{3}{2}})(1599) j_1[(8/3)^{1/2}y_D]$$

$$- \sqrt{3}(1599) j_1[(\sqrt{\tfrac{4}{3}})y_D] + 1627 j_1(2y_D)\}, \quad (33)$$

$$L_2 = \frac{5}{1309}\int_0^{y_D} \{224 j_2(y) + 453 j_2[(8/3)^{1/2}y]$$

$$- 288 j_2[(\sqrt{\tfrac{4}{3}})y] - 262 j_2(2y)\}y^2 dy, \quad (34)$$

and the zero-point optical-phonon contribution is

$$F_{\mathrm{op}}{}^0 = \tfrac{1}{2}D_{\mathrm{op}}[(\omega_t/\omega_l + 2)L_1 + (\omega_t/\omega_l - 1)L_2]. \quad (35)$$

We have defined

$$y_D = k_D R, \quad (36)$$

and k_D is given by Eq. (17). The unitless constant D_{op} in Eqs. (32) and (35) is

$$D_{\mathrm{op}} = \frac{8\pi}{3}\frac{g\mu_B \langle S_z\rangle}{H_c}\left(\frac{ee'}{R^6}\right)^2 \sum_{n,n'} U_{nn'} \frac{1496\hbar}{5103\rho\pi^2}\frac{1}{R\omega_t}$$

$$= \frac{D_{\mathrm{ac}}}{2}\left(\frac{\hbar}{k_B}\right)^2\left(\frac{v_t}{R}\right)^3 \frac{1}{\omega_t}. \quad (37)$$

Contributions to the hyperfine constant from the various branches are additive, so that the final expression for $A(T)$ becomes

$$A(T) = A(0)\{1 - [F_{\mathrm{ac}}{}^0 + \sum_r^{n-1}(F_{\mathrm{op}}{}^0)_r]$$

$$- [F_{\mathrm{ac}}(T) + \sum_r^{n-1}(F_{\mathrm{op}}(T))_r]\}. \quad (38)$$

C. Comparison with Previous Results

By expanding the expressions[16] for $j_n(\rho)$ about $\rho = 0$, we obtain

$$j_0(\rho) \to 1 - \frac{\rho^2}{6} + \frac{\rho^4}{120} - \cdots, \quad j_2(\rho) \to \frac{\rho^2}{15} - \frac{\rho^4}{210} + \cdots. \quad (39)$$

Substitution of these expansions into Eqs. (25) and (26) yields

$$F_{\mathrm{ac}}(T) \to CT^6 \int_0^{\Theta'/T} x^5[(e^x - 1)]^{-1}dx, \quad (40)$$

TABLE III. Values of the parameters for CaF_2, SrF_2, and BaF_2.

Host	R (Å)	v_l (10^5 cm/sec)	v_t (10^5 cm/sec)	ρ (g/cm³)	$\omega_l(1)$[a] (10^{13} Hz)	$\omega_t(1)$[a] (10^{13} Hz)	$\omega_l(2)=\omega_t(2)$[a] (10^{13} Hz)	Θ (°K)	Θ' (°K)
CaF_2	2.37[b]	7.36[c]	3.34[c]	3.21[c]	8.72[d]	4.84[d]	6.07[e]	508[c]	352
SrF_2	2.51[b]	5.46[f]	2.92[f]	4.32[f]	7.05[d]	4.09[d]	5.28[g]	380[f]	264
BaF_2	2.69[b]	4.48[h]	2.30[h]	4.89[h]	6.14[d]	3.47[d]	4.58[g]	282[h]	196

[a] (1) refers to the infrared-active and (2) to the Raman-active optical branch.
[b] R. W. G. Wyckoff, *Crystal Structures* (Wiley-Interscience Inc., New York, 1963), 2nd ed., Vol. 1.
[c] D. R. Huffman and M. H. Norwood, Phys. Rev. **117**, 709 (1960).
[d] W. Kaiser, W. G. Spitzer, R. H. Kaiser, and L. E. Howarth, Phys. Rev. **127**, 1950 (1962).
[e] R. S. Krishman and N. Krishnamurthy, J. Phys. (Paris) **26**, 633 (1965).
[f] D. Gerlich, Phys. Rev. **136**, A1366 (1964).
[g] I. Richman, Phys. Rev. **133**, A1364 (1964).
[h] D. Gerlich, Phys. Rev. **135**, A1331 (1964).

where

$$C=\frac{8\pi}{3}\frac{g\mu_\beta\langle S_z\rangle}{H_c}\left(\frac{ee'}{R^3}\right)^2\sum_{n,n'}U_{nn'}\frac{(32)(53)\hbar}{(81)(343)\rho\pi^2}$$

$$\times\left(\frac{2}{3v_t^7}+\frac{1}{v_l^7}\right)\left(\frac{k_B}{\hbar}\right)^6, \quad (41)$$

in exact agreement with Eqs. (17) and (18) of Ref. 9. In addition, by expanding the sine and cosine terms in Eq. (27) to seventh order in the argument, it can be shown that

$$F_{ac}^0\to\tfrac{1}{12}C\Theta'^6. \quad (42)$$

Thus, except for our use of Θ' here instead of Θ, the equations for the acoustic branch obtained from the improved theory reduce to the correct limiting expressions in the long-wavelength ($kR\ll1$) approximation for all temperatures T. No equations for the optical branch have been derived in this approximation.

To investigate the limit $kR\gg1$, we use[16]

$$j_n(\rho)\xrightarrow[\rho\to\infty]{}(1/\rho)\cos[\rho-\tfrac{1}{2}(n+1)\pi], \quad (43)$$

which is valid for $\rho>\tfrac{1}{2}n(n+1)$. Substitution of Eq. (43) into Eqs. (24)–(26) yields terms of the form

$$T^2\int_0^{\Theta'/T}\left(x+\sum_{\sigma,i}\frac{C_i^\sigma}{T}\sin\rho_i^\sigma\right)(e^x-1)^{-1}dx, \quad (44)$$

where the C_i^σ are constants and the ρ_i^σ are defined in Eq. (20) for $i=0, \cdots, 3$. Although no calculation has been performed for the rare-earth ions in the approximation $kR\gg1$, it is clear that the usual short-wavelength treatment,[6] in which the quantity in Eq. (3) is regarded as a constant, would yield only the first term in Eq. (44). Consequently, the expressions derived from the short-wavelength approximation are not directly recovered from the improved treatment. It can be shown that the coefficients C_i^σ/T of the nonrecoverable terms are negligible in CaF_2 only for $T\gg260°$K.

III. COMPARISON WITH EXPERIMENT

A. Temperature Dependence of Hyperfine Constant

Measurements of the hyperfine coupling constant as a function of temperature have been made[9,10] on $^{151}Eu^{2+}$ in CaF_2, SrF_2, and BaF_2. The data were analyzed on the basis of the long-wavelength Debye theory given by Eqs. (40) and (41), in which only the acoustic branch was included, and where the experimental values of Θ (not Θ') were employed. We reanalyze these data now on the basis of the improved theory. Since $n=3$ for the alkaline-earth fluorides, we include one acoustic and two optical branches, of which the first is the infrared-active and the second is the Raman-active branch. The values of the parameters appropriate to the three host crystals are presented in Table III. Hartree-Fock-Slater calculations of Eu^{2+} orbitals were used[9] to evaluate $U_{nn'}$ and the sum $\sum_{n,n'}$ was restricted to $n=n'=6$.

In Fig. 1. are plotted the experimental values[9,10] of the hyperfine constant as a function of temperature for the three samples. Best-fit values of D_{ac} and C, called
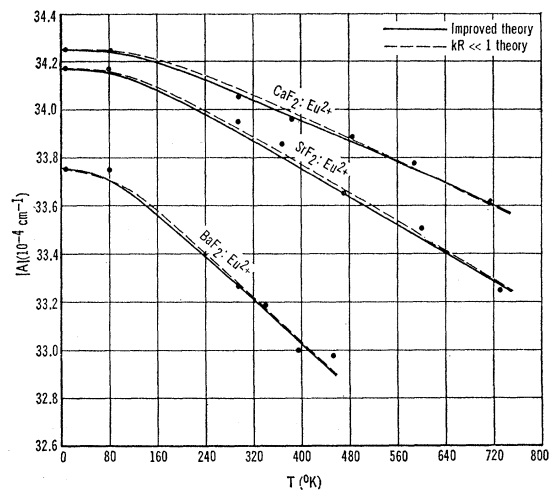

FIG. 1. Temperature dependence of the hyperfine constant of $^{151}Eu^{2+}$ in CaF_2, SrF_2, and BaF_2. Solid dots are the experimental data, the solid curve is the improved, and the dashed curve is the approximate theory, using the best-fit values D_{ac}^{expt} and C^{expt} for the constants.

TABLE IV. Experimental and theoretical values of D_{ac} and C for Eu^{2+} in CaF_2, SrF_2, and BaF_2.

Host	$10^8 D_{ac}^{expt}$ $(°K)^{-2}$	$10^{10} D_{ac}^{theor}$ $(°K)^{-2}$	$D_{ac}^{expt}/D_{ac}^{theor}$	$10^{18} C^{expt}$ $(°K)^{-6}$	$10^{19} C^{theor}$ $(°K)^{-6}$	C^{expt}/C^{theor}
CaF_2	7.46 ± 1.65	7.58	98.4	5.31 ± 1.23	5.85	9.1
SrF_2	14.8 ± 1.8	4.73	313	28.1 ± 4.1	7.92	35.5
BaF_2	35.2 ± 8.7	4.44	793	203 ± 60	25.2	80.5

D_{ac}^{expt} and C^{expt}, were determined from the experimental data. These values were used to calculate $A(T)$ for both the improved and the long-wavelength theories that appear in Fig. 1 as solid and dashed curves, respectively. It is interesting that both models produce nearly the same temperature dependence for the hyperfine constant and both fall well within the error limits (not displayed in Fig. 1) of the experimental data. Hence it appears that no significant improvement in the functional dependence of A on T is achieved by the improved treatment.

Theoretical values of D_{ac} and C, called D_{ac}^{theor} and C^{theor}, were calculated from Eqs. (30) and (41), respectively, using the parameters listed in Table III. Their values, as well as those of D_{ac}^{expt} and C^{expt}, are recorded in Table IV for Eu^{2+} in the three alkaline-earth-fluoride samples. Also recorded in Table IV are the ratios of the experimental to the theoretical values of these coefficients for the two models. For all three hosts and both models, the theoretical values of the coefficients are too small, but the disparity is actually greater for the improved model. One possible reason for the greater disparity is that in the long-wavelength model one employs the small argument expansions of the sine and cosine functions, and these approximations are always in such a direction as to overestimate the value of the function. Hence, the magnitude of C^{theor} is enhanced with respect to D_{ac}^{theor}, the value obtained when these functions are treated exactly. Whether or not this is a sufficient reason to cause the improved treatment to disagree with experiment by about a factor 10 more than the approximate treatment is not certain. In any case, the improved theory is of course the more correct one, and its inability to predict the correct magnitude of the effect is quite apparent. Also note that, although the percentage error in the values of D_{ac}^{expt} is generally smaller than that in C^{expt}, the difference is not great enough to represent a significant improvement in the qualitative fit to the data (Fig. 1).

It must be pointed out that only the value of D_{ac} was adjusted to produce the best fit with the experimental data, and that the ratio of the optical to the acoustic contribution was regarded as fixed by the expression (37). According to this relationship, we found that the optical contribution at room temperature was 25% for the CaF_2 crystal, 30% for SrF_2, and 23% for BaF_2. Again, while it is not anticipated that the use of D_{op} as a second adjustable parameter would have greatly improved the qualitative fit to the data, it is quite possible

that it might have reduced the discrepancy between the experimental and calculated magnitudes of the effect. Nevertheless, it is believed that restricting the theory to only one arbitrary parameter is a more meaningful approach.

It can be seen from Table IV that the disagreement between the experimental and calculated values of the coefficients in both the improved and approximate models increases with increasing atomic number of the host cation. However, whereas C^{expt} increases as well as C^{theor} (although not at the same rate as C^{expt}) as one proceeds down the column of the table, D_{ac}^{theor} decreases while D_{ac}^{expt} increases. Consequently, some features of the long-wavelength model which initially appeared encouraging[10] are in fact deceptive, since the improved model yields results whose magnitude and trends are grossly different.

B. Rigid-Lattice Values of Hyperfine Constant

The zero-point contribution ΔA_{ZP} to the hyperfine coupling constant is determined by the relation

$$\Delta A_{ZP} = -A(0)(F_{ac}^0 + F_{op}^0), \quad (45)$$

where F_{ac}^0 and F_{op}^0 are given by Eqs. (27) and (35) in the improved model and F_{ac}^0 is given by Eq. (42), with Θ' replaced by Θ, in the long-wavelength model. Then the "rigid-lattice" value A_{RL} is

$$A_{RL} = A(0) - \Delta A_{ZP}. \quad (46)$$

Listed in Table V are the values of ΔA_{ZP} and A_{RL} for both the improved and long-wavelength models calculated by using D_{ac}^{expt} and C^{expt}, respectively. Note that the rigid-lattice values for the three host crystals are not equal, even when the error limits are included, and that the value of A_{RL} in BaF_2 is considerably lower than those of SrF_2 and CaF_2. Also, there is rather close agreement between the values of A_{RL} determined from the two models.

It is interesting that the optical-phonon contributions to ΔA_{ZP} in the exact model are 42, 51, and 46% for Eu^{2+} in CaF_2, SrF_2, and BaF_2, respectively. These contributions are much greater than those determined at room temperature and indicate that optical phonons cannot be neglected in zero-point calculations.

IV. CONCLUSIONS

We would like to summarize the advancements made by our exact treatment of spatial averaging in the orbit-

lattice interaction. In the past, separate and independent calculations based on either the long- or short-wavelength approximation have been performed for both the spin-lattice relaxation time[1,7] and the temperature dependence of the hyperfine coupling constant.[5,6,9] In all of these calculations, the range of validity of the approximation used was a pertinent but unanswered question. We wish to emphasize that this question has not been answered here; instead, we have obviated the the necessity of asking it. In addition, our calculation encompasses, without approximation, the phonon-wavelength region $kR \approx 1$, which has never been treated before.

The improved theory for the temperature-dependent hyperfine constant demonstrates that some of the results obtained from the long-wavelength theory are in fact spurious. For example, since the improved treatment predicts a decrease in the magnitude of the effect with increasing atomic weight of the host cation, it is only fortuitous that the long-wavelength approximation predicts an increase in this magnitude and that such an increase is observed experimentally. Consequently, the theory based on the long-wavelength approximation can be misleading when used to determine the systematics of A for various ions in different crystalline hosts.

We have also shown that the expressions for the hyperfine constant generally derived from the short-wavelength approximation[6] cannot be exactly recovered from the present theory, whereas the new equations reduce exactly to their former expressions[9] in the long-wavelength limit.

Calculations of the zero-point contribution and rigid-lattice value of the hyperfine constant of Eu^{2+} in the three host materials have also been made. Unlike those of Mn^{2+} in the oxides,[12] the values of A_{RL} for Eu^{2+} in the alkaline-earth fluorides are not equal, and their differences lie outside the error limits.

Finally, the improved theory for the temperature dependence of the hyperfine coupling constant of rare-earth S-state ions in cubic crystals appears to provide no better qualitative fit to the data than the theory derived from the long-wavelength approximation. However, perhaps the thermodynamic nature of the phenomenon being studied, as well as the small (approximately 2 or 3%) changes in A measured over a 700°K temperature range, disguises the improvement in the model. It is expected that the improvement should be much more visible when applied to spin-lattice relaxation times which are sensitive functions of temperature.

More important is the fact that the predicted magnitude of the effect is in serious disagreement with ex-

TABLE V. Zero-point and rigid-lattice values of the hyperfine constant (in 10^{-4} cm^{-1}) from both the improved and approximate models for Eu^{2+} in CaF_2, SrF_2, and BaF_2.

Host	Improved model		Long-wavelength model	
	ΔA_{ZP}	A_{RL}	ΔA_{ZP}	A_{RL}
CaF_2	0.185 ± 0.041	-34.43 ± 0.09	0.261 ± 0.061	-34.51 ± 0.11
SrF_2	0.201 ± 0.025	-34.37 ± 0.08	0.241 ± 0.036	-34.41 ± 0.10
BaF_2	0.239 ± 0.059	-33.99 ± 0.11	0.287 ± 0.085	-34.04 ± 0.14

periment. Of course, the improved theory has not yet been applied to the temperature-dependent hyperfine constant of iron-group S-state ions in cubic crystals, and hence it is uncertain how universal this result is, but calculations for these systems will be presented in the near future. It must also be remembered that lattice-expansion effects on the temperature dependence of A have been ignored in this work because of the absence of the experimental data, but we assume that such effects are negligible.[13,17,18] In any case, it is clear that the inadequacy of the theory can no longer be attributed to the much-suspected use of the long- or short-wavelength approximations, which is important to know so that attention can now be given to some of the other weaknesses mentioned in Sec. I. Of these, the use of the point-charge model is probably the most important, although this model is expected to be representative for the inner-shell $4f$ electrons of rare-earth ions. Apparently, covalency and overlap cannot be neglected in calculations of this type.[11]

Also suspect are the Debye and Einstein approximations for the phonon spectrum of the crystal. To use the correct eigenvectors and eigenvalues of the lattice would obviously be a superior approach, but these are, of course, unknown. However, since a directional averaging procedure valid over the whole phonon-wavelength range is now available, it is possible that the diatomic linear chain[12,13] or some similar model can now be employed to greater advantage than the Debye or Einstein models.

ACKNOWLEDGMENTS

[17] J. Rosenthal and L. Yarmus, J. Chem. Phys. **46**, 1217 (1967).
[18] J. Rosenthal, L. Yarmus, and R. H. Bartram, Phys. Rev. **153**, 407 (1967).